Vol. 32: 251–259, 2003 | AQUATIC MICROBIAL ECOLOGY
Aquat Microb Ecol | Published July 14

Morphometric variability of the genus *Nodularia* (Cyanobacteria) in Baltic natural communities

Roberta Congestri*, Enrico Capucci, Patrizia Albertano

Department of Biology, University of Rome 'Tor Vergata', Via della Ricerca Scientifica, 00133 Rome, Italy

ABSTRACT: Morphometric variability of the filamentous diazotroph *Nodularia* was determined in natural, mixed-species samples during a summer cyanobacterial bloom in the Central Baltic Sea using epifluorescence microscopy coupled with image analysis. A total of 1350 cyanobacterial filament images were acquired and a number of morphometric parameters measured for individual trichomes present in the samples and used to distinguish *Nodularia* from *Aphanizomenon* and *Anabaena*. The approach allowed automatic estimates of linear dimensions of *Nodularia*, *Aphanizomenon* and *Anabaena*, enabling us to evaluate their biovolume and vertical distribution, and to observe a high degree of morphometric variability in *Nodularia* filaments. We statistically analyzed this phenotypic diversity using previously collected datasets and adding further measurements. The data obtained were used to assess the variability in *Nodularia* trichome width and morphology and to establish the possible existence of 3 *Nodularia* 'morphotypes' by discriminant analysis.

KEY WORDS: Nodularia · Morphometry · Image analysis · Discriminant analysis · Baltic Sea

INTRODUCTION

Blooms of diazotrophic cyanobacteria occur regularly throughout summer in the Baltic Sea. Heterocystous filaments of *Nodularia*, *Aphanizomenon* and *Anabaena* coexist within the summer cyanobacterial assemblage together with picoplanktonic unicells. The latter can contribute as much as 80% of total cyanobacterial biomass and 50% of total primary production in this period of the year (Stal et al. 1999, Stal & Walsby 2000). The filamentous fraction is the most obvious, with buoyant trichomes and colonies floating up to the uppermost water layer to benefit from the higher irradiance. Large areas of surface aggregates, eventually forming scums, become visible to the naked eye (Kahru et al. 1994, Walsby et al. 1995).

Massive cyanobacterial growth is favoured by the onset of calm, stratified conditions induced by the increase in water temperature and nitrogen depletion (low DIN:DIP ratios) along the water column (Niemi 1979, Kononen et al. 1996). Generally, these conditions occur in July/August after the spring bloom, when combined nitrogen sources are depleted (Kononen et al. 1996, Stal et al. 1999), triggering the growth of heterocystous cyanobacterial species able to fix nitrogen from the atmosphere, and outcompeting non-diazotrophic microorganisms.

Recently, image analysis methods based on phycobiliprotein autofluorescence have been developed to calculate the contribution of various heterocystous genera to the total cyanobacterial biomass in natural samples (Congestri et al. 2000). Computer mediated methods are also known to provide precise estimates of the linear dimensions of filamentous cyanobacteria (Walsby & Avery 1996), and of cell abundance and the morphometric variability of picoplanktonic chroococcaleans (Albertano et al. 1997). These methods could be useful tools in monitoring bloom forming taxa, especially those associated with toxin production. Baltic *Nodularia* strains have been shown to produce nodularin, a hepatotoxic cyclic pentapeptide which can act as a liver tumor promoter and direct carcinogen (Carmichael et al. 1988, Sivonen et al. 1989). Extensive blooms of *Nodularia* are globally distributed in the

*Email: roberta.congestri@uniroma2.it

brackish environments of the world (Sellner 1997, Bolch et al. 1999, Moisander & Pearl 2000), arousing public concern over their potential toxicity. In recent years, long-term data showed increasing trends in bloom quantity and intensity in the Baltic Basin (Finni et al. 2001).

In this study we further tested the method based on epifluorescence microscopy combined with image analysis, as described by Congestri et al. (2000). The approach allowed automatic estimates of linear dimensions of all the heterocystous cyanobacterial genera present in the samples collected during summer 1999 in the Central Baltic Sea. Morphometric datasets of our previous work for each cyanobacterial genus are statistically analyzed in the present paper. Here we focus on *Nodularia* morphometry. This genus shows the largest variability, leading us to hypothesize a distinction between cell diameter classes within the natural assemblage. This hypothesis was statistically analyzed by discriminant analysis based on an extra dataset collected on *Nodularia* heterocyst morphometry. The presence of at least 2 distinct and more frequent morphotypes was statistically evidenced. This distinction seemed consistent with the traditional taxonomic assessment of Baltic *Nodularia* that discriminates between different species on the basis of the morphologic traits of the filaments (Komárek et al. 1993), but is in conflict with recent molecular data that indicate the existence of one species only (Barker et al. 2000a). In any case, our approach allowed automated or semi-automated analysis of the cyanobacterial community structure, thus contributing to a morphologic and morphometric characterization of taxa in natural assemblages, avoiding the loss of diacritical morphologic features and genotypic selection occurring in laboratory culture.

MATERIALS AND METHODS

Samples were collected during 3 (Stns 12–14) 24 h experiments (6/7, 8/9 and 10/11 July 1998) at a drift station in the South Gotland Sea (Baltic Sea), 56°18 N, 19°05 E, on RV 'Alexander von Humboldt' (Baltic Sea Research Institute, Warnemünde, Germany).

A 100 µm-mesh closing plankton net was towed vertically through the 0–7, 7–14 and 14–21 m depth layers, at 04:00, 12:00, 20:00, 24:00, 04:00 h (local time), over the 3 diel cycles. Aliquots of concentrated seawater samples, each resulting from 10 net tows at different depth intervals, were fixed on board in 2.5% glutaraldehyde, diluted in filtered seawater, and kept in 15 ml tubes at 4°C. A total of 45 samples were collected and transferred to the laboratory.

Some preliminary observations were conducted in light and epifluorescence microscopy (Leica M2 green filter set, excitation wavelength 546 nm, cut-off at 580 nm) to evaluate the composition of the microphytoplanktonic community and the morphology of the diazotrophic cyanobacterial genera present in the samples.

In order to estimate the morphometry of the heterocystous cyanobacteria, the samples were processed by means of epifluorescence microscopy coupled with a Quantimet automatic system equipped with an image analysis software, as reported in Congestri et al. (2000).

Statistics were applied primarily to the width datasets of *Nodularia*, *Aphanizomenon* and *Anabaena*, obtained by processing a total of 1350 images. Frequency and descriptive procedures of the SPSS package for Windows were used to analyze class frequency distribution and descriptive statistics of the 3 genera, separately. Each individual genus dataset was first considered as a whole and then pooled according to day, time and depth of sampling.

To further analyze *Nodularia* morphometric variability, 100 out of 1000 images were randomly selected from *Nodularia* .tif files previously stored (Congestri et al. 2000), with the aim of distinguishing between the different morphotypes. Each randomly selected filament was assigned *a priori* to Type 1, 2 or 3 according to the trichome morphology evident in epifluorescence microscopy. Morphometry of 225 heterocysts present in these trichomes was evaluated after manual circumscribing them (tracing lines with a mouse along the *Nodularia* filaments) to determine estimates of width, length, area and perimeter of the highlighted heterocysts. At least 2 heterocysts per filament were measured. When no overlapping or crossing of filaments was present, 3 heterocysts were measured. Heterocyst manual circumscription was conducted using greater magnification in order to achieve a more precise automatic measurement with the image analysis software. Based on *a priori* classification of filament types, a discriminant analysis was then performed (using the 'Classify; discriminant' procedure of the SPSS package) to construct a predictive model of group membership using the heterocyst morphometric data. This procedure generated linear combinations of the predictor variables which provided the best discrimination between the groups. The functions were constructed from a randomly selected sample consisting of 50% of the dataset from known groups whose group membership was known. Then we applied the functions to the remaining 50% to cross-validate the consistency between the *a priori* classification of types (1, 2, 3) and the one using the functions.

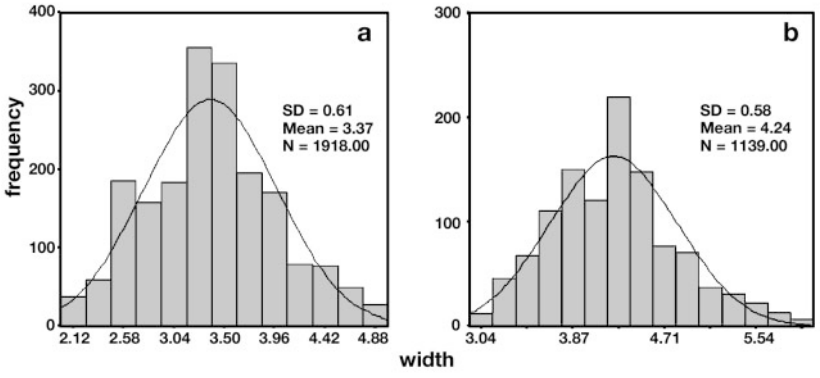

Fig. 1. Frequency distribution of width data, expressed in µm, for (a) *Anabaena* and (b) *Aphanizomenon* recorded in the samples

RESULTS

Nodularia, *Aphanizomenon* and *Anabaena* filaments, along with the centric diatoms *Chaetoceros*, *Skeletonema* and *Thalassiosira* spp., and dinoflagellates such as *Dinophysis* and *Phalacroma* spp. primarily contributed to the structure and composition of the microphytoplanktonic community sampled at the drift station in the South Gotland Sea in July 1998.

The possible interference signals due to phycoerythrin contained in *Dinophysis norvegica* and *D. acuminata* (Carpenter et al. 1995, Hewes et al. 1998) did not hinder cyanobacterial filament resolution under the epifluorescence illumination used during image recording.

Descriptive and frequency analysis conducted on the width datasets of *Aphanizomenon* and *Anabaena*, separately, was not able to distinguish different width classes. Class frequency distributions were almost normal (Fig. 1a,b), as shown by histograms pertaining to *Aphanizomenon* and *Anabaena*. *Nodularia* class frequency distributions represented marked deviations from the Gaussian curve. They indicated multimodal patterns both when considering the dataset as a whole or when pooled according to different depths and stations (Fig. 2) and time of sampling (Fig. 3). The Kolmogorov-Smirnov test of normality was then applied to test the hypothesis that the datasets were normally distributed. Results indicated that *Nodularia* distributions differed significantly from the normal distribution (Table 1).

This deviation suggested the possibility of distinguishing more than one diameter class in the *Nodularia* natural assemblage, as also hypothesized during epifluorescence observations. In fact, 3 different morphotypes distinguishable on the basis of their width and other morphologic traits were found to coexist in the recorded images (ca. 1000) containing *Nodularia* filaments. The 3 'morphotypes' appeared in epifluorescence microscopy as follows: a wider and more common type, labelled as Type 3 (Fig. 4a,b,e), showed individual cells easily visible along the trichome because of the presence of discernible cross-

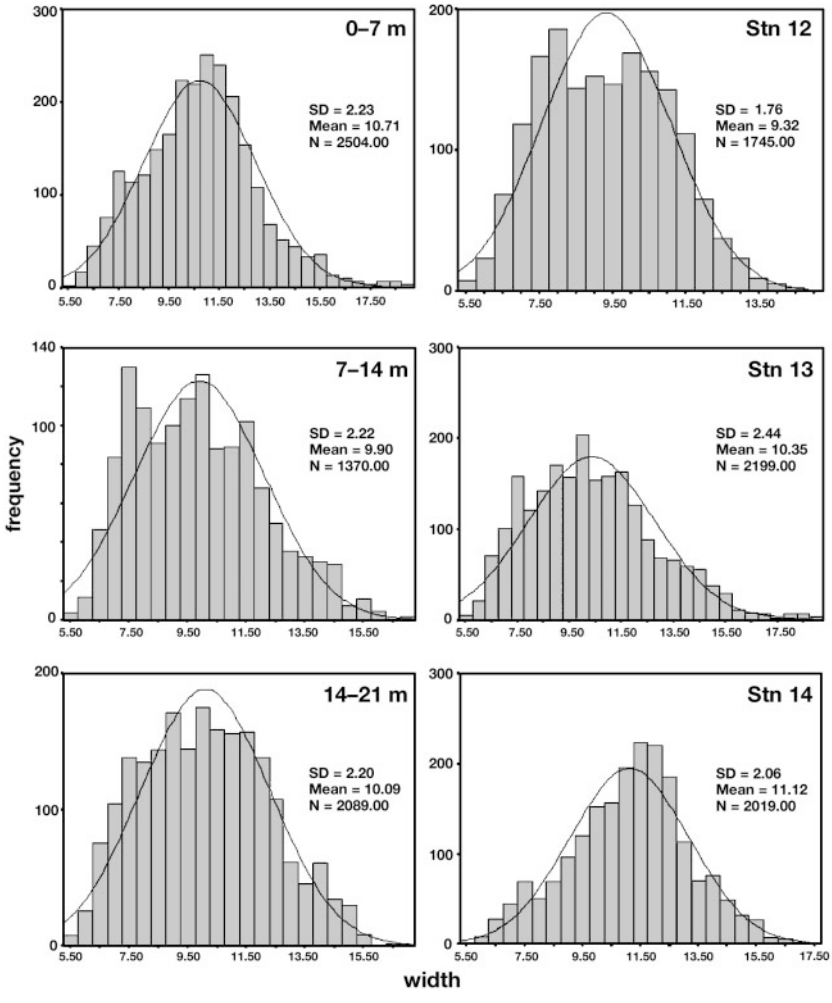

Fig. 2. *Nodularia.* Frequency distribution of width data, expressed in µm, at 3 different depths (0–7, 7–14 and 14–21 m) and stations (Stns 12, 13 and 14) of sampling

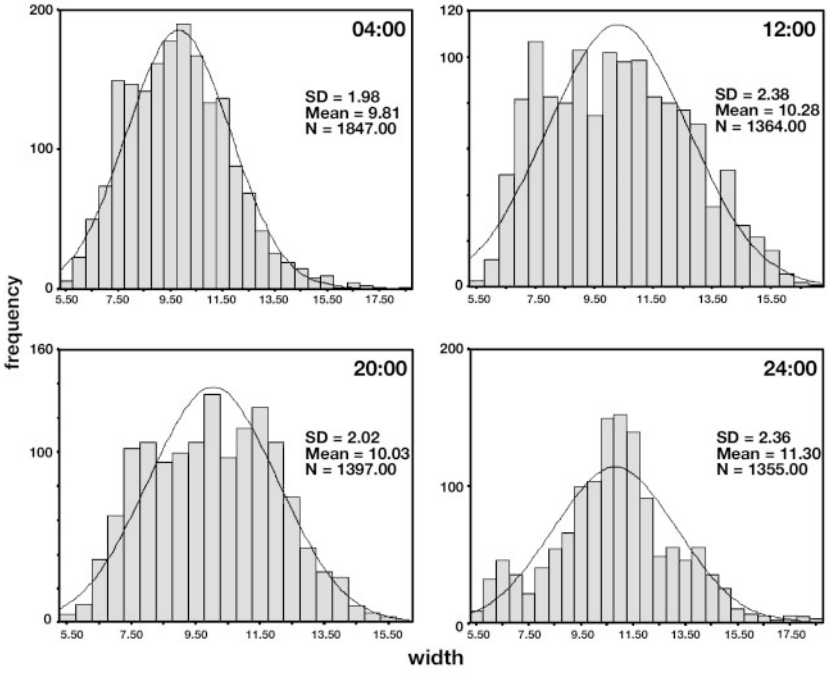

Fig. 3. *Nodularia.* Frequency distribution of width data, expressed in µm, at different times (04:00, 12:00, 20:00 and 24:00 h) of sampling

walls. Filaments were usually straight or slightly curved. The length:width ratio of the vegetative cells was barely measurable due to the presence of cross-walls forming in almost every cell. A narrower type, Type 2 (Fig. 4a,c,d), showed short discoid vegetative cells and barely visible cross-walls. Filaments were usually spirally entangled. A third and rather rare type, Type 1 (Fig. 4a,e,f), formed tightly coiled filaments. The heterocysts were oval in shape and visibly wider than vegetative cells, the latter still being the narrowest.

Table 1. *Nodularia.* Results of the Kolmogorov-Smirnov (K-S) test of normality applied to width data pooled according to different stations, depths and time of sampling. Significance values (p) less than 0.05 indicated that distribution differed significantly from a normal distribution

		K-S statistic	df	p
Station	12	0.063	1745	0.000
	13	0.046	2199	0.000
	14	0.040	2019	0.000
Depth (m)	7	0.037	2504	0.000
	14	0.044	2089	0.000
	21	0.061	1370	0.000
Time	04:00	0.036	1847	0.000
	12:00	0.063	1364	0.000
	20:00	0.053	1397	0.000
	24:00	0.051	1355	0.000

A discriminant analysis was performed in order to build a predictive model based on microscopical observations and the multimodal patterns revealed by descriptive and frequency procedures. For this purpose, 100 images were randomly selected among those containing *Nodularia* trichomes and each filament was *a priori* assigned to a morphologic type. In addition, automatic measurement of the *Nodularia* filament widths was calculated and stored. Morphometry, namely the length, width, area and perimeter of the heterocysts present along the selected filaments, was evaluated and subsequently used to construct a discriminant function. No akinetes were observed in the filaments, so the heterocyst morphometric traits provided the independent measurements necessary for membership grouping. It is known that *Nodularia* heterocysts retain their thylakoids for a long time (Šmarda et al. 1988). This retention allowed us to distinguish the heterocysts under epifluorescence illumination, and to assume that the measured heterocyst population was at the same developmental stage. A total of 225 heterocysts were measured along the filaments, 53 of which were attributed to Type 3, 34 to Type 2 and 13 to Type 1. This also suggested the relative proportion of the different types in the natural samples. Type 3 was confirmed to be the most common in the samples, Type 2 showed an intermediate frequency and Type 1 was the rarest encountered.

Discriminant analysis allowed coefficients of the linear discriminant functions to be estimated (Table 2). The functions were applied to the subset of cases used to construct the functions themselves. *A posteriori* classification, based on the predictor variables, matched the original *a priori* grouping of filament types

Table 2. *Nodularia.* Coefficients of the Fisher's linear discriminant functions estimated using heterocyst morphometric data of *a priori* classified filament types (1, 2, 3)

	Type 1	Type 2	Type 3
Area	−1.303	−1.358	−1.544
Perimeter	5.780	5.659	6.416
Length	−1.216	6.670E−02	0.673
Width	11.736	12.006	13.378
(Constant)	−63.408	−70.149	−95.250

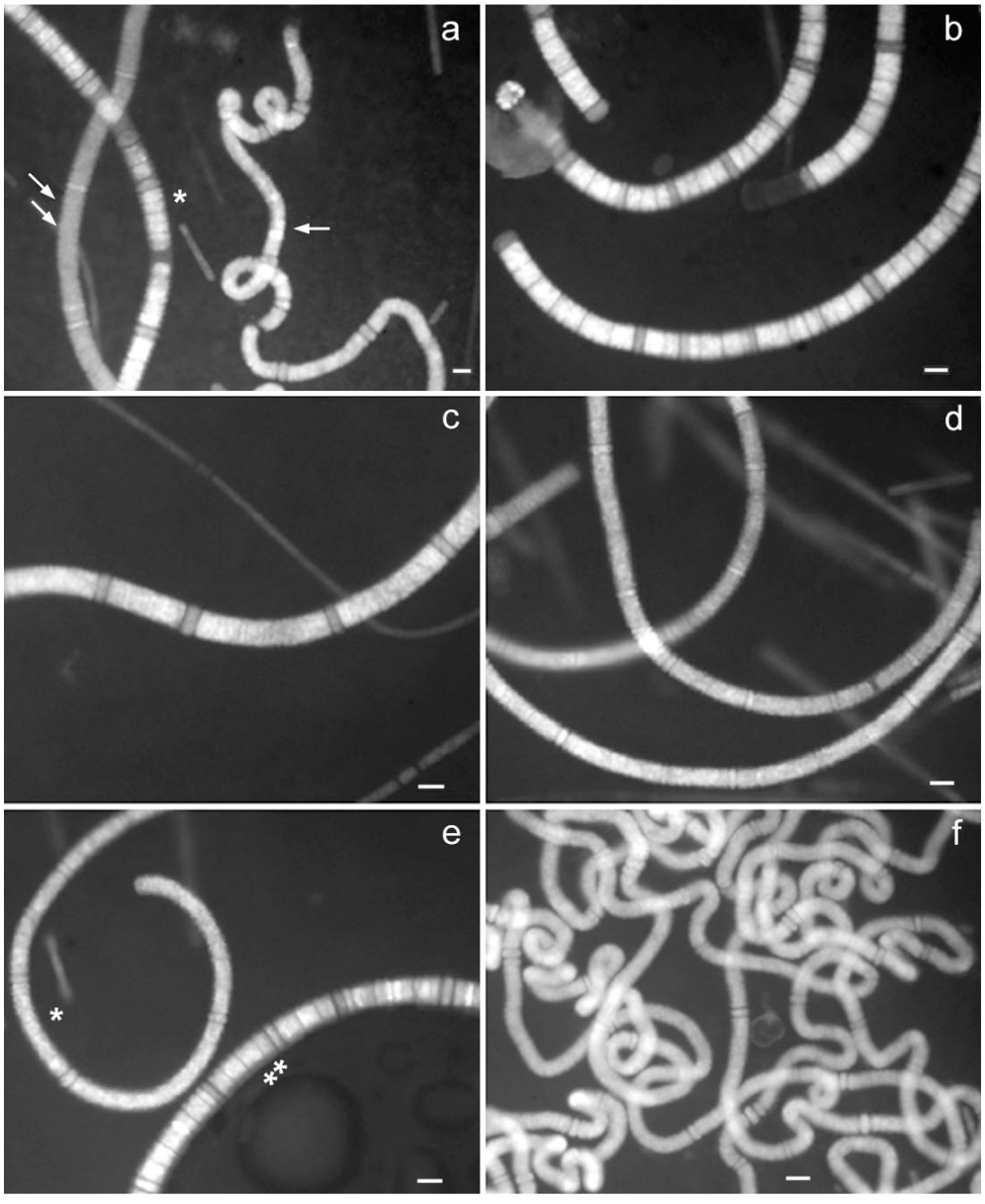

Fig. 4. *Nodularia.* Epifluorescence recorded images of the 3 morphotypes observed in the samples. Type 1 filaments (a: arrow; e: asterisk; and f) of 7, 7.7 and 8 µm widths, respectively. Type 2 filaments (a: double arrow; c; and d) of 10.7, 10.9 and 8.9 µm widths, respectively. Type 3 filaments (a: asterisk; b; and e: double asterisk) of 12.5, 11.2 and 11.7 µm widths, respectively. Scale bars = 10 µm

in 84% of the cases (Table 3). When the functions were applied to the 50% not selected to construct the functions, in order to cross-validate the *a posteriori* classification, the percentage was 80. In Table 3 we also report the classification results for each filament type, both for selected and unselected subsets of data. The functions correctly discriminated Type 3 in 91% of the cases and Type 2 in 87%, but appeared unable to discriminate filaments belonging to Type 1 because of their attribution to Type 2 in 80% of the cases. The scatterplot of combined groups (Fig. 5) is constructed on the basis of canonical discriminant functions, whose coefficients are reported in Table 4. Evidence here shows that Function 1 (mostly correlated with length, perimeter and area, Table 5) clearly separated Type 3 from Type 2 and 1. Conversely, Type 1 and 2 filaments were not clearly distinguished, although Type 1 was localized towards the lowest values of the Function 1 axis. Function 2, mostly correlated to width (Table 5), did not provide any evidence of discrimination between the groups.

Table 3. Classification results obtained applying the discriminant functions to the subsets of cases selected and not selected for their construction. In all, 84.4% of selected original grouped cases were correctly classified, and 80.0% of unselected original grouped cases were correctly classified

		Predicted membership			
	Type	1	2	3	Total
Cases selected					
Original count	1	1	9	0	10
	2	1	28	7	36
	3	0	1	67	68
Percentage	1	10.0	90.0	0	100.0
	2	2.8	77.8	19.4	100.0
	3	0	1.5	98.5	100.0
Cases not selected					
Original count	1	3	12	0	15
	2	1	34	4	39
	3	0	5	51	56
Percentage	1	20.0	80.0	0	100.0
	2	2.6	87.2	10.3	100.0
	3	0	8.9	91.1	100.0

Using this function we were able to statistically discriminate 2 different morphometric types in the 100 randomly selected *Nodularia* filaments; one corresponded to Type 3 filaments, the other encompassed routined Type 2 and 1 trichomes. This result may be significant in terms of the *Nodularia* assemblage sampled, implying that it can be considered typical of the entire natural community. Therefore this provides a description of the phenotypic diversity of this cyanobacterial genus in the late summer bloom community. Also, at least 2 different and more frequent morphotypes were shown to coexist in the field.

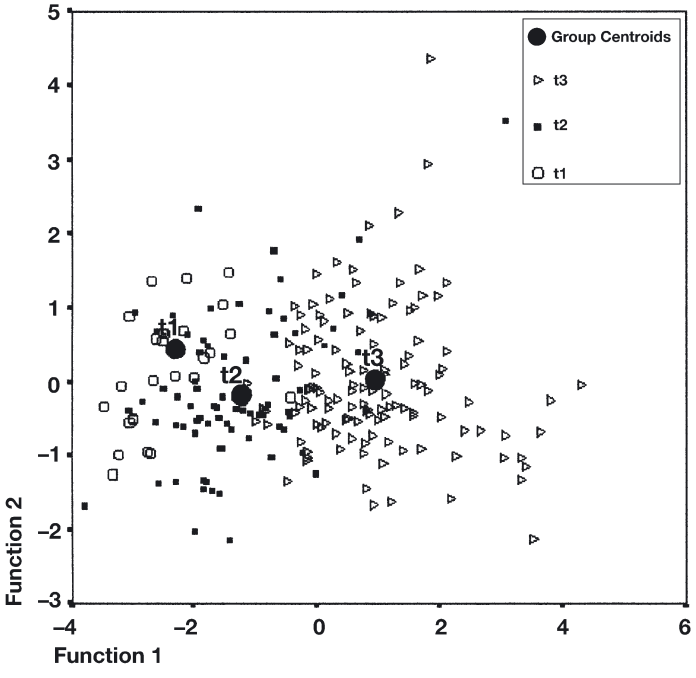

Fig. 5. *Nodularia.* Scatterplot of the 3 combined showing distribution of morphotypes and their group centroids

Table 4. Coefficients of the 2 standardized canonical discriminant functions used for the scatterplot in Fig. 5

	Function	
	1	2
Area	−2.639	−1.693
Perimeter	1.706	4.150
Length	0.900	−2.974
Width	0.705	0.685

Table 5. Correlations between discriminating variables and standardized canonical discriminant functions. Variables ordered by absolute size of correlation within function. *Largest absolute correlation between each variable and any discriminant function

	Function	
	1	2
Length	0.735*	−0.022
Perimeter	0.621*	0.251
Area	0.357*	0.333
Width	0.311	0.644*

Measurement of the trichome/cell diameter, conducted on the 100 randomly selected *Nodularia* images, allowed us to further characterize the 3 types of filaments classified *a priori* during epifluorescence observation. The width of Type 3 filaments ranged from 11.1 to 18.8 µm, with a mean of 13.5 µm (SD = 1.8 and 0.2 µm), while Type 2 ranged from 7.7 to 12.7 µm and the mean was 10 µm (SD = 1.3 and 0.2 µm). It has to be pointed out that only 2 Type 2 filaments of 7 to 8 µm were observed out of 34. Type 1 width range was lower than the others, between 7.2 and 8.8 µm, with a mean of 8.1 µm (SD = 0.55 and 0.2 µm). Nevertheless, during the previous image processing (Congestri et al. 2000), some filaments of ca. 6 µm attributable to Type 1 were observed, although they were not randomly selected for the purpose of the present work.

DISCUSSION

Traditional cytomorphologic analysis and, to a lesser extent, ecological characters have long been used to classify natural cyanobacterial populations. In addition, the application of biometrical methods to sets of parameters provided reliable results, especially when linear dimensions (quantitative characters) were used to discriminate the different forms at genus and spe-

cies level (Hoffmann 1988, Komárková 1988, Komárek & Kováčik 1989, Bazzichelli & Abdelahad 1994). The problem in finding limits in the distribution of the differentiating criteria within communities, so as to separate them into non-overlapping classes, makes it necessary to combine studies on natural and cultural material. Culture studies provided further characters to delineate species such as the physiological, biochemical and genetic variability of different strains. Therefore, the combination of traditional, chemotaxonomic and molecular approaches seemed promising for describing communities, populations and species diversity. However, in some cases this was a problem since molecular and genetic data, mostly based on the analysis of the 16S rRNA sequences, indicated that morphologic characters do not necessarily result in a phylogenetically reliable taxonomy (Wilmotte 1994). Furthermore, it was not always possible to combine different data into a meaningful taxonomic assessment, since the morphologic data did not always consistently reflect the similarities observed in the gene sequence. This was the case with the Baltic *Nodularia* (Hayes & Barker 1997, Barker et al. 1999, Lehtimäki et al. 2000, Laamanen et al. 2001), the taxonomic status of which is currently being questioned. Three planktonic species have been described from Baltic isolates and field material, *Nodularia litorea*, *N. spumigena* and *N. baltica* (Komárek et al. 1993), on the basis of the traditional morphologic approach (morphology of the different types of cells, presence of gas vesicles, ultrastructural features), nodularin production and ecological characteristics. Further studies reported the presence of only the former 2 species in natural *Nodularia* assemblages (Walsby et al. 1995, Albertano et al. 1996). However, another form was less frequently observed which did not correspond to any of the previously recognized taxa (Walsby et al. 1995). By coupling genetic and morphologic data on 6 Baltic strains, the coexistence of distinct *Nodularia* species was confirmed, namely *N. spumigena* and *N. sphaerocarpa*, along with another isolate not currently described in any of the established taxa (Bolch et al. 1999). Conversely, other studies suggested an inconsistency between phenotypic and genotypic features for the purpose of congruency and accurate species delineation (Barker et al. 1999, Lehetimäki et al. 2000, Laamanen et al. 2001). A recent population genetic study revealed a high degree of genetic heterogeneity within 12 different genotypes, whose distribution demonstrated the occurrence of horizontal gene flow ultimately implying that a single 'species' does exist in the Baltic Sea (Barker et al. 2000a). This was later supported by Laamanen et al. (2001), who coupled genetic and phenotypic approaches with the aim of finding morphologic or molecular markers in order to discriminate between toxic and non-toxic strains of *Nodularia* in the field.

In the present study the application of discriminant analysis to the automatic datasets showed a clear-cut separation between 2 *Nodularia* groupings within the Baltic natural community. Despite the general consensus on the continuum represented by the morphologic variation of Baltic *Nodularia*, the discriminant function allowed statistical groupings of all *Nodularia* morphometric data into at least 2 distinct morphometric entities. Although the function was not able to clearly separate Type 1 from Type 2, the calculated ranges of trichome diameter for these morphotypes did not show any overlap, both when considering the mean values ±SE or SD (mean ± SD: Type 1 = 7.5–8.6, Type 2 = 8.7–11.3). Thus, it was possible to infer that 2 *Nodularia* morphotypes co-occurred during cyanobacterial bloom formation in late summer in the Baltic Sea. These can be defined on the basis of the general morphology, trichome width and heterocyst morphometry. Whether these types represent different growth forms of a single *Nodularia* species related to the environmental conditions, nutrient status or life cycle stages cannot be ruled out. However, it is known that these 'forms' belonged to an actively growing assemblage that has been exposed to the same local environmental conditions and experienced N-starvation and N-repleteness during the bloom formation observed (Gallon et al. 2002). The doubling of biomass between 6 and 11 July 1998 (Gallon et al. 2002), the lack of akinetes and the presence of mostly fluorescent heterocysts in our samples would indicate that the *Nodularia* filaments were presumably at the same stage of development. We considered them as units of morphologic/morphometric diversity, irrespective of their still-questionable biological significance. In any case, one morphotype, Type 3, resembled the filament morphology reported for *N. litorea* (Kutz.) Thuret (Komárek et al. 1993). *N. litorea* is described as (9.5) 10–15 (18) µm wide, with straight or curved trichomes, constricted at cross walls and characterized by very short, barrel-shape cells, with discoid heterocysts of the same width as that of vegetative cells. Type 2, although not statistically separated from Type 1, resembled *N. spumigena* Mertens characterized by straight, curved, spiral and coiled trichomes of (6) 6.8–12 (16) µm in width, constricted at cross walls and with discoid, cylindrical or barrel-shape cells and transversely oval heterocysts. Therefore, 2 of the morphotypes statistically distinguished in this study shared some morphologic features with species described on the basis of a classical taxonomic revision (Komárek et al. 1993), though no correspondence was found between the degree of filament coiling observed by us and that reported in the literature as a diacritical feature.

The taxonomic assessment of Type 1 was another problem, although it resembled *Nodularia baltica* in heterocyst morphology, the latter being transversely oval to almost spherical and wider than vegetative cells. Further observations indicated that the tightly coiled filaments assigned to Type 1 could be statistically distinguished from Type 2 using our discriminant function .

Our aim was, therefore, to show an application of the image analysis-based method we developed in order to estimate filamentous cyanobacterial biomass in mixed-species natural assemblages.

Population genetic analysis of *Nodularia* partially carried out over the same area and period revealed that 3 out of the 12 allele-combinations distributed across the Baltic Sea were much more frequent than others (Barker et al. 2000a). These data suggest a correlation between the 3 genotypes and the 3 morphotypes observed by us. However, the frequency distribution reported for the 3 most abundant genotypes did not match that of our 3 morphotypes of *Nodularia.*

Using this system, the width distribution pattern of *Aphanizomenon* appeared to be rather close to normal and is confirmed by the most recent molecular data on the genotypic homogeneity of the Baltic *Aphanizomenon* population. This is considered to be clonal and not attributable to the species *A. flos-aquae* (Barker et al. 2000b), as indicated by Janson et al. (1994) on the basis of ultrastructural data.

Future application of this function could be used for a rapid morphometric assessment of natural *Nodularia* assemblage. It would be especially useful in fully automatic systems where highlighting of heterocysts in the filament would allow the automatic calculation of their linear dimensions.

Acknowledgements. We gratefully thank Dr. Maria Lo Ponte for improving the English in this manuscript and Dr. Palma Mattioli for her skillful assistance during image analysis processing. This work is a contribution to the European Union ELOISE Programme (ELOISE No. 377/15) within the framework of the BASIC project carried out under contract ENV4-CT97-0571.

LITERATURE CITED

Albertano P, Di Somma S, Leonardi D, Canini A, Grilli Caiola M (1996) Cell structure of planktic cyanobacteria in the Baltic Sea. Arch Hydrobiol Suppl Algol Stud 83:29–54

Albertano P, Di Somma S, Capucci E (1997) Cyanobacterial picoplankton from the Central Baltic Sea: cell size classification by image-analyzed fluorescence microscopy. J Plankton Res 19 (10):1405–1416

Barker GLA, Hayes PK, O'Mahony SL, Vacharapiyasophon P, Walsby AE (1999) A molecular and phenotypic analysis of *Nodularia* (Cyanobacteria) from the Baltic Sea. J Phycol 35:931–937

Barker GLA, Handley BA, Vacharapiyasophon P, Stevens JR, Hayes PK (2000a) Allele-specific PCR shows that genetic exchange occurs among genetically diverse *Nodularia* (Cyanobacteria) filaments in the Baltic Sea. Microbiology 146:2865–2875

Barker GLA, Konopka A, Handley BA, Hayes PK (2000b) Genetic variation in *Aphanizomenon* (Cyanobacteria) colonies from the Baltic Sea and North America. J Phycol 36:947–950

Bazzichelli G, Abdelahad (1994) Caractérisation morphométrique et statistique de deux populations d'*Aphanizomenon* du groupe *Aphanizomenon ovalisporum* Forti des lacs de Nemi et Albano (Italie). Arch Hydrobiol/Suppl Algol Stud 73:1–21

Bolch CJS, Orr PT, Jones GJ, Blackburn SI (1999) Genetic, morphologic, and toxicological variation among globally distributed strains of *Nodularia* (Cyanobacteria). J Phycol 35:339–355

Carmichael WW, Eschedor JT, Patterson JML, Moore RE (1988) Toxicity and partial structure of a hepatotoxic peptide produced by the cyanobacterium *Nodularia spumigena* Mertens emend. L575 from New Zealand. Appl Environ Microbiol 54 (9):2257–2263

Carpenter EJ, Janson S, Boje R, Pollehne F, Chang J (1995) The dinoflagellate *Dinophysis norvegica*: biological and ecological observations in the Baltic Sea. Eur J Phycol 30: 1–9

Congestri R, Federici R, Albertano P (2000) Evaluating biomass of Baltic filamentous cyanobacteria by image analysis. Aquat Microb Ecol 22:283–290

Finni T, Kononen K, Olsonen R, Wallström K (2001) The history of cyanobacterial blooms in the Baltic Sea. Ambio 30 (4–5):172–178

Gallon JR, Evans AM, Jones DA, Albertano P and 14 others (2002) Maximum rates of N_2 fixation and primary production are out of phase in a developing cyanobacterial bloom in the Baltic Sea. Limnol Oceanogr 47(5): 1514–1521

Hayes PK, Barker GLA (1997) Genetic diversity within Baltic Sea populations of *Nodularia* (Cyanobacteria). J Phycol 33:919–923

Hewes CD, Mitchell BG, Moisan TA, Vernet M, Reid FMH (1998) The phycobilin signatures of chloroplasts from three dinoflagellate species: a microanalytical study of *Dinophysis caudata*, *D. fortii*, and *D. acuminata* (Dinophysiales, Dinophyceae). J Phycol 34:945–951

Hoffmann L (1988) Criteria for the classification of blue-green algae (cyanobacteria) at the genus and at the species level. Arch Hydrobiol/Suppl Algol Stud 50–53:131–139

Janson S, Carpenter EJ, Bergman B (1994) Fine structure and immunolocalisation of proteins in *Aphanizomenon* sp. from the Baltic Sea. Eur J Phycol 29:203–211

Kahru K, Horstman U, Rud O (1994) Satellite detection of increased cyanobacterial blooms in the Baltic Sea: natural fluctuation or ecosystem change? Ambio 23:469–472

Komárek J, Kováčik L (1989) Trichome structure of four *Aphanizomenon* taxa (*Cyanophyceae*) from Czechoslovakia, with notes on the taxonomy and delimitation of the genus. Plant Syst Evol 164:47–64

Komárek J, Hübel M, Hübel H, Šmarda J (1993) The *Nodularia* studies 2. Taxonomy. Arch Hydrobiol/Suppl Algol Stud 68:1–25

Komárková J (1988) Morphologic variation in natural populations of *Anabaena lemmermannii* in respect to the existence of *Anabaena utermoehlii*. Arch Hydrobiol/Suppl Algol Stud 50–53:93–108

Kononen K, Kuparinen J, Mäkelä K, Laanemets J, Pavelson J,

Nõmmann S (1996) Initiation of cyanobacterial blooms in a frontal region at the entrance to the Gulf of Finland, Baltic Sea. Limnol Oceanogr 41(1):98–112

Laamanen MJ, Gugger MF, Lehtimäki J, Haukka K, Sivonen K (2001) Diversity of toxic and nontoxic *Nodularia* isolates (Cyanobacteria) and filaments from the Baltic Sea. Appl Environ Microbiol 67 (10):4638–4647

Lehtimäki J, Lyra C, Suomalainen S, Sundman P, Rouhiainen L, Paulin L, Salkinoja-Salonen M, Sivonen K (2000) Characterization of *Nodularia* strains, cyanobacteria from brackish waters, by genotypic and phenotypic methods. Int J Syst Evol Microbiol 50:1043–1053

Moisander PH, Pearl HW (2000) Growth, primary productivity, and nitrogen fixation potential of *Nodularia* spp. (Cyanophyceae) in water from a subtropical estuary in the United States. J Phycol 36:645–658

Niemi A (1979) Blue-green algal blooms and N:P ratio in the Baltic Sea. Acta Bot Fenn 110:57–61

Sellner KG (1997) Physiology, ecology, and toxic properties of marine cyanobacteria blooms. Limnol Oceanogr 42 (5): 1089–1104

Sivonen K, Kononen K, Carmichael WW, Dalhem AM, Rinehart KL, Kiviranta J, Niemelä SI (1989) Occurrence of the hepatotoxic cyanobacterium *Nodularia spumigena* in the Baltic Sea and structure of the toxin. Appl Environ Microbiol 55:1990–1995

Šmarda J, Komárek J, Čáslavská J, Hübel M (1988) The *Nodularia* studies 1. Introduction, fine structure. Arch Hydrobiol/Suppl Algol Stud 50–53:109–129

Stal LJ, Walsby AE (2000) Photosynthesis and nitrogen fixation in a cyanobacterial bloom in the Baltic Sea. Eur J Phycol 35:97–108

Stal LJ, Staal M, Villbrandt M (1999) Nutrient control of cyanobacterial blooms in the Baltic Sea. Aquat Microb Ecol 18:165–173

Walsby AE, Avery A (1996) Measurement of filamentous cyanobacteria by image analysis. J Microbiol Methods 26: 11–20

Walsby AE, Hayes PK, Boje R (1995) The gas vesicles, buoyancy and vertical distribution of cyanobacteria in the Baltic Sea. Eur J Phycol 30:87–94

Wilmotte A (1994) Molecular evolution and taxonomy of the cyanobacteria. In: Bryant DA (ed) The molecular biology of cyanobacteria. Kluwer Academic, Dordrecht, p 1–25

Editorial responsibility: William Li, Dartmouth, Nova Scotia, Canada

Submitted: January 25, 2002; Accepted: April 23, 2003
Proofs received from author(s): July 4, 2003